Proceedings of the 1996 IEEE
International Conference on Robotics and Automation
Minneapolis, Minnesota - April 1996

Modeling and Analysis of Dynamic Contact Point Sensing by a Flexible Beam

M. M. Svinin, N. Ueno, M. Kaneko, T. Tsuji
Industrial and System Engineering Department,
Faculty of Engineering, Hiroshima University,
Higashi-Hiroshima 739, Japan

Abstract

A dynamic active antenna sensor for locating a contact point is considered in this paper. In its simpliest realization the sensor can be implemented in the form of a flexible beam rotating in plane. The main feature of the sensor is the use of the frequency-contact point curve which, for some regions, may be a multi-valued function. One way of "improving" the curve could be concerned with the non-uniform mass and stiffness distribution of the beam, which would lead to a rather complicated sensor design. Another way to remedy the situation is to change the sensing strategy by adding a proper control action at the joint of the beam. To study the sensor's response to the control, a dynamic model of the beam in contact with the external environment is developed. Analysis of the frequency equation shows how a simple proportional control law changes the sensing curve. It is found that in some limiting, but practically attainable cases the sensing curve becomes a single-valued function. Thus, the solution proposed can significantly simplify the identification procedure.

1 Introduction

Invention of many sensors being currently used in robotics and mechatronics was inspired by existance of "similar" devices in living creatures. Observing behavoir of insects, which in a sense can be thought of as prototypes of mobile robots, one cannot help noting the skill they use their antennae to avoid hitting objects particulary close to them. An interesting observation is that insects are always moving their flexible antennae actively when they are crawling, runnung, and even staying still.

This observation led Kaneko [1] to developing a new class of sensors for detecting a contact point. The main features of this type of sensors, named Active Antenna, are flexibility of the probing tool and ability to move it actively. These features as well as working principles for the Active Antenna were discussed in [2]. In its simpliest realization the Active Antenna can be represented by an actuator rotating a straight flexible beam in a plane. The role of the curvature of the beam shape in the sensing process was analyzed in [2]. Extension of the concept to the spatial 3D case has been done in [3]. A survey of related to the Active Antenna contact sensors can be found in [2], where they are classified from the viewpoint of active and passive sensing.

Initially, the concept of the Active Antenna has been presented for the static conditions of sensing. In this case a small motion is imparted at the joint and the information about the contact point can be extracted from a torque sensor mounted at the antenna's base. Later on, the concept of active sensing has been extended to the dynamic formulation [4, 5]. In the dynamic case motions of the beam are separated into the searching phase and the detecting phase. The latter is further separated into the contact phase and non-contact phase. The moment the beam hits an object the reaction torque is changing impulsively, and therefore the corresponding contact angle can be detected. The actuator is stopped right after the moment the contact has ben detected. Free oscillations of the beam, resulting from the contact (impact), are excited and measured through the torque sensor. As has been proved in [6], the coordinate of the contact point is defined uniquely from a given spectrum of the natural frequencies of the beam in the contact phase.

Generally, it is not desirable to alternate the contact and non-contact phases during the sensing process. In other words, it is necessary to prevent the antenna from bouncing and repeating collisions, which is possible only with relatively fast identification of the contact point. Thus, the dynamics of the contact phase imposes severe restrictions on the sensing time, limiting

0-7803-2988-4/96 $4.00 © 1996 IEEE

it in a rough approximation to half a period of the fundamental oscillation. Unfortunately, for the uniform beam the sensing curve—the natural frequency versus the contact point—is not a single-valued function of the frequency [4, 5]. Therefore, the higher order frequencies must be brought into the analysis, which of course complicates the identification procedure.

To exclude the multivalence region from the sensing curve, one can try to change the mass and the stiffness distribution for the beam. One possible solution is to attach a concentrated mass to the tip of the beam [4]. Increasing the mass reduces the multivalence range and, in the limiting case, shifts it to the right end of the curve. Designing the beam with a variable cross-section with linear tapering leads to the same effect [6]. Both these design solutions are hardly attractive from the viewpoint of practical applicability. In the first case, the gravity effects may complicate functioning of the antenna. Moreover, for relatively high values of the mass the physical picture of the impact phenomena may be changed if the contact is made at the tip point. In the second case the cross-section has unusual form, widening from the base to the end of beam.

Another, radically different way to remedy the situation is to change the sensing strategy itself. The original formulation of the sensing strategy has one disadvantage. Indeed, by fixing the actuator in the moment of contact we impose an additional constraint, which makes the system stiffer. Relaxing the constraint and letting the joint of the beam move in accordance with a control law during the sensing process may increase the fundamental period of oscillations and ease the identification procedure.

Analysis of the sensing curve is based upon a sufficiently accurate mathematical model of the beam. In the research community there has been a great deal of interest in the modeling and control of single-link flexible arms [7]. In spite of the fact that the literature on the topic is voluminous, very few publications covered dynamics and force control of the beam in contact with the environment. Most relevant to our problem are works [8,9], where the eigenfunction expansion was considered for the tip contact condition. Impact analysis was conducted in [10], where oscillations were excited by hitting a concentrated mass attached to the tip of the beam. Thus, the models for a middle-point-contact have not been given considerable attention in literature. Finally, an important difference between our research problem and conventional control problems should be clarified. The difference is in regarding vibration—we are not interested in damping it out, we use it as an information source.

This paper is organized as follows. Firstly, in Section 2, the dynamic model of the sensor is presented. Next, in Section ??, a solution for the dynamic equations is obtained. After that, in Section 3, an analysis of the frequency equation is undertaken. Here, it is shown how the sensing curve can became a single-valued function of the fundamental frequency, which essentially simplifies the identification procesure. Some practical recommendations and theoretical research problems resulting from our approach are discussed in Section 4. Finally, conclusions are drawn in Section 5.

2 Dynamic Model of the Sensor

The sensor is modeled as a flexible beam having a point-contact with environment, as shown in Fig. 1. A rotating frame OX_hY_h is attached to the hub. The beam is clamped at the hub, and its elastic transversal displacements $v(x,t)$ are measured with respect to the beam's axis OY_h. Let J_h be the inertia moment of the hub, q_h the rotation angle, and τ_h the applied torque. The flexible link is assumed to be uniform, of length L, with constant Young's modulus E, area moment of inertia I about the bending axis, and mass per unit length μ. A payload of mass m_p is attached to the tip of the beam.

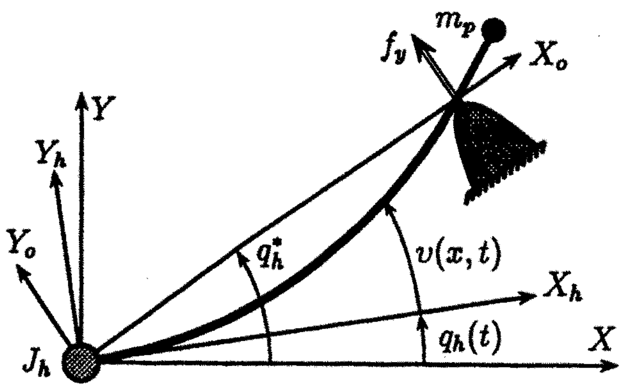

Figure 1: Flexible beam in contact phase.

The following common assumptions are made in the mathematical model: the beam rotates in a horizontal plane so that gravitational effects are not included; the angular velocity of the beam is much less than the lowest natural frequency of the beam; rotatory inertia and shear deformation are neglected; the radius of joint and payload are neglected; friction in the joint and internal friction of the beam are neglected.

The coordinates of an arbitrary point of the beam in the inertial reference frame OXY are defined as follows

$$X(x,t) = x\cos q_h - v(x,t)\sin q_h, \quad (1)$$
$$Y(x,t) = x\sin q_h + v(x,t)\cos q_h. \quad (2)$$

Let q_h^* be the contact angle, and $l \in [0, L]$ be the contact distance. As to the environment formalization, we assume the following. The object does not move during the sensing, and sliding of the contacting bodies relative to one another is negligible for the duration of the impact. Friction at the contact point is negligible so that the longitudinal contact forces are not included in the model. Under these assumptions, the virtual displacement at the contact point, expressed in the axes OX_hY_h, must be zero. Therefore, the constraint imposed onto the beam's motion can be formalized as

$$S(l,t) = lq_h + v(l,t) = \text{const} = lq_h^*, \quad (3)$$

where $S(l,t)$ has the meaning of length of the contact arc.

The kinetic energy T of the system is the sum of kinetic energies of the hub T_h, the beam T_b, and the payload T_p, where

$$T_b = \frac{1}{2}\int_0^L \mu(\dot{X}^2(x,t) + \dot{Y}^2(x,t))dx, \quad (4)$$
$$T_p = \frac{1}{2}m_p(\dot{X}^2(L,t) + \dot{Y}^2(L,t)), \; T_h = \frac{1}{2}J_h\dot{q}_h^2. \quad (5)$$

Here and throughout the paper, dots are used to denote time differentiation, and primes to denote partial differentiation with respect to x. The potential energy, accounting for the distributed elasticity, and the virtual work of the non-conservative forces are given by

$$P = \frac{1}{2}\int_0^L EI(v''(x,t))^2 dx, \quad (6)$$
$$\delta W = \delta q_h \tau_h + (\delta v(l,t) + l\delta q_h)f_y, \quad (7)$$

where f_y is the contact force between the beam and the object. This force can be interpreted as a Lagrange multiplier (normal reaction) associated with the constraint (3). The Hamilton's Extended Principle, $\int_{t_1}^{t_2}(\delta T - \delta P + \delta W)dt = 0$, is used to derive the dynamics equations. This Principle leads to the following equation for the virtual displacements

$$\delta q_h\{\tau_h + lf_y - J\ddot{q}_h - \int_0^L \mu\ddot{v}(x,t)x dx - m_pL\ddot{v}(L,t)\}$$
$$-\delta v(x,t)\int_0^L (EIv''''(x,t) + \mu\ddot{v}(x,t) + \mu\ddot{q}_h x)dx$$
$$+\{EIv'''(x,t)\delta v(x,t) - EIv''(x,t)\delta v'(x,t)\}_0^L$$
$$-\delta v(L,t)\{m_p(\ddot{v}(L,t) + L\ddot{q}_h)\} + \delta v(l,t)f_y = 0, \quad (8)$$

where $J = J_h + J_b + J_p$, $J_b = \mu L^3/3$, and $J_p = m_pL^2$. The geometric boundary conditions are defined as $v(0,t) = 0$ and $v'(0,t) = 0$. Motion equations and the dynamic boundary conditions follow from (8). They, however, explicitely depend on the contact force f_y. To exclude the contact force and simplify the analysis, the following transformation of variables is introduced

$$\theta(t) = q_h(t) - q_h^*, \quad u(x,t) = v(x,t) + x\theta(t). \quad (9)$$

Upon transforming the virtual work equation (8) and the constraint equation (3) to the new variables, after simplifications one obtains the following linear equations of motion and boundary conditions:

$$J_h\ddot{\theta} - EIu''(0,t) = \tau_h, \quad (10)$$
$$EIu''''(x,t) + \mu\ddot{u}(x,t) = 0, \quad (11)$$
$$u(0,t) = 0, u'(0,t) = \theta, u''(L,t) = 0, \quad (12)$$
$$u(l,t) = 0, \; EIu'''(L,t) = m_p\ddot{u}(L,t). \quad (13)$$

The choice of the control action τ_h defines a sensing strategy. One possible action is to impose an additional constraint $\theta = 0$. This corresponds to a passive sensing strategy. Another possible strategy, which can be called active, is to set $\tau_h = 0$ for the time of sensing action. Limiting ourselves to the linear models and simple design solutions, we choose

$$\tau_h = -k\theta, \quad (14)$$

where k is the static feedback gain. The control (14) can be interpreted as an artificial active compliance acting at the joint.

3 Analysis of the Frequency Equation

Equations (10-13) with control (14) can be solved using the classical method of separation of variables. For the n-th vibration mode, the shape functions $\varphi_n(x)$ and the natural frequencies ω_n are defined from the following eigenvalue problem:

$$\varphi''''(x) - \lambda^4\varphi(x) = 0, \quad (15)$$

$$\varphi(0) = 0, \varphi(l) = 0, \varphi''(L) = 0, \tag{16}$$
$$(J_h\omega^2 - k)\varphi'(0) + EI\varphi''(0) = 0, \tag{17}$$
$$EI\varphi'''(L) + m_p\omega^2\varphi(L) = 0, \tag{18}$$

where $\lambda^4 = \mu\omega^2/EI$. Let $z = l/L$ be the normalized coordinate of the contact point, and $\beta = \lambda L$.

Written for the dimensionless variable β, the frequency equation for the system under consideration can be represented in the following form

$$\left(\frac{J_h}{3J_b}\beta^4 - \frac{kL}{EI}\right)\psi_c(\beta) - \beta\psi_p(\beta) = 0, \tag{19}$$

where $\psi_c(\beta)$ and $\psi_p(\beta)$ are the left-hand sides of the frequency equations corresponding, respectively, to the "clamped-free" case and to the "pinned-free" case with $J_h = 0$ and $k = 0$. In a sense, they are basis functions for the frequency analysis. These basis functions are derived as

$$\psi_c(\beta) = \psi_{co}(\beta) + \frac{m_p}{m_b}\beta\psi_{cm}(\beta), \tag{20}$$

$$\psi_p(\beta) = \psi_{po}(\beta) + \frac{m_p}{m_b}\beta\psi_{pm}(\beta), \tag{21}$$

with the explicit analytical representation given by

$$\psi_{co}(\beta) = \frac{1}{4}\{\cosh\beta(1-z)[\sin\beta\cosh\beta z - \sin\beta(1-z)] + \cos\beta(1-z)[\sinh\beta(1-z) - \sinh\beta\cos\beta z] + \cosh\beta z\sin\beta z - \cos\beta z\sinh\beta z\}, \tag{22}$$

$$\psi_{cm}(\beta) = \frac{1}{8}\{2\sin\beta\sinh\beta - 4\sin\beta(1-z)\sinh\beta(1-z) + \cos\beta\cosh\beta(1-2z) - \cosh\beta\cos\beta(1-2z) + \sin\beta\sinh\beta(1-2z) + \sinh\beta\sin\beta(1-2z)\}, \tag{23}$$

$$\psi_{po}(\beta) = \frac{1}{4}\{[\cos\beta(1-z) + \cosh\beta(1-z)][\sin\beta\cdot\sinh\beta z + \sinh\beta\sin\beta z] - [\sin\beta(1-z) + \sinh\beta(1-z)][\cos\beta\sinh\beta z + \cosh\beta\sin\beta z]\}, \tag{24}$$

$$\psi_{cm}(\beta) = \frac{1}{2}\{\sin\beta\sinh\beta z\sinh\beta(1-z) - \sin\beta(1-z)\sin\beta z\sinh\beta\}. \tag{25}$$

It is to be noted that $\psi_c(0) = 0$ and $\psi_p(0) = 0$. Also, for $z = 0$ $\psi_c(\beta) = 0, \psi_p(\beta) = 0$. In this case the physical system tends to the classical "clamped-free" case with no intermediate support, and the frequency equation transforms to $1 + \cosh\beta\cos\beta + \beta m_p(\cos\beta\sinh\beta - \sin\beta\cosh\beta)/m_b = 0$. If the contact point is $z = 1$ the frequency equation does not depend on m_p, with the basis functions becoming $\psi_c(\beta) = (\sin\beta\cosh\beta - \cos\beta\sinh\beta)/2$ and $\psi_p(\beta) = \sin\beta\sinh\beta$.

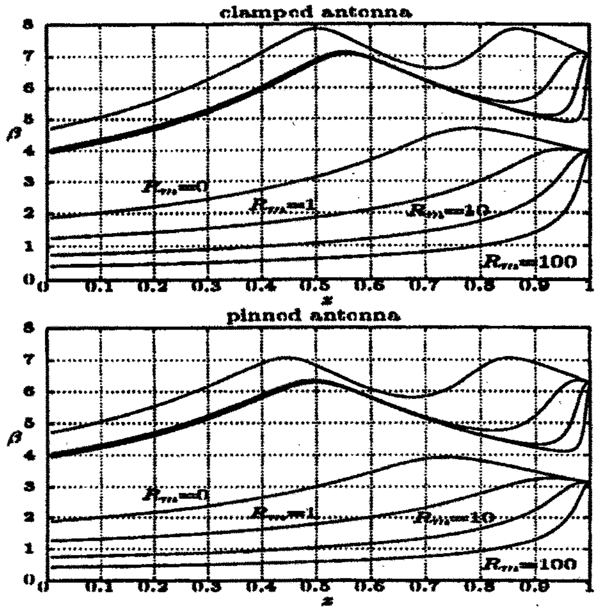

Figure 2: Sensing curve.

Let us define the following three parameters

$$R_J = J_h/J_b,\ R_s = kL/EI,\ R_m = m_p/m_b, \tag{26}$$

where R_J is the ratio of the moment inertia of the hub to that of the beam, R_s is the ratio of the torsional stiffness to the bending stiffness of the beam, EI/L, and R_m is the ratio of the mass of the payload to that of the beam, $m_b = \mu L$. As can be seen, the frequency analysis is fully defined in terms of these three ratios. For instance, the basis functions $\psi_c(\beta)$ and $\psi_p(\beta)$ result from the limiting cases of $R_J \to \infty \bigvee R_s \to \infty$ and $R_J \to 0 \bigwedge R_s \to 0$.

To study properties of the sensing curve for the limiting cases, a set of simulations is conducted. Figure 2 shows two first frequencies of the limiting models as functions of contact point z, with mass ratio R_m changing from 0 to 100. As can be seen, the region of doublevalence of β_1 is larger for the pinned model. To identify the contact point uniquely it is necessary to use an addtitional information coming from either the normalized amplitudes or the higher order frequencies.

Now, let us examine the case of $R_J \neq 0$ and $R_s = 0, R_m = 0$. Figure 3 shows behavior of the sensing

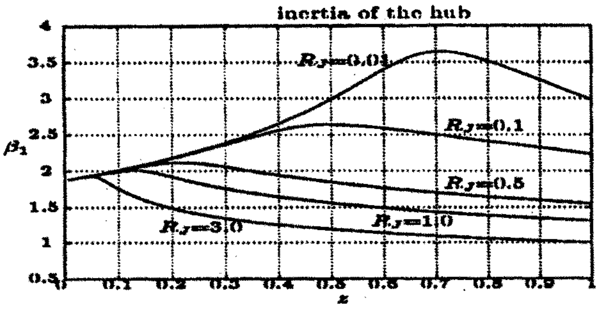

Figure 3: Sensing curve.

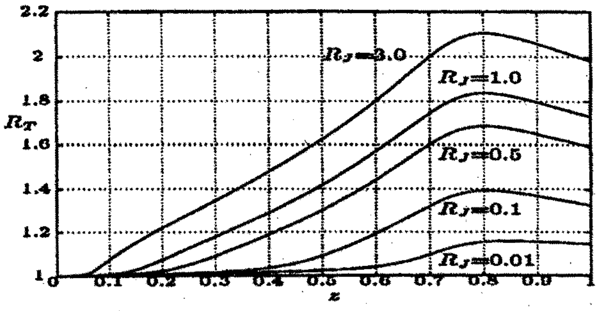

Figure 4: Ratio of fundamental periods.

curve for the inertia ratio R_J changing from 0 to 3. As can be seen, taking R_J into consideration leads to appearance of yet another natural frequency, and this frequency becomes the fundamental one. The behavior of this frequency is quite different from that of the system with $R_J = 0$. One attractive feature is that this frequency is significantly lower than that of the models for the "clamped-free" and the "pinned-free" cases. And this is to the advantage of the identification procedure, since the fundamental period is increasing. Figure 4 shows the change of the time ratio $R_T = T/T_c$. Another important feature is that that with increasing R_J the interval of the doublevalence is becoming shorter and is shifting to the beginning of the curvature. Thus, with relatively high values of R_J we can shift the doublevalence region to the non-working range of the sensor*. Note, however, that with increasing R_J the fundamental frequency tends to zero as the ridid-body mode becoming dominant. To prevent this situation and keep the fundamental frequency on a certain level, the stiffness ratio R_s must be increased as well.

To better understand the role of R_s, let us finally examine the limiting case of a massless beam, i.e., when $R_m \to \infty$. To this end, we rewrite the frequency equation as

$$\left(\frac{J_h}{3J_b}\beta^4 - \frac{kL}{EI}\right) = \beta\frac{\psi_p(\beta)}{\psi_c(\beta)}, \tag{27}$$

and note that $\mu = \beta^4 EI/L^4\omega^2$. Taking into account that μ and β have different rates of convergence to zero, it is easily derived from (27) that

$$\frac{L}{EI}(J_h\omega^2 - k) = \lim_{\beta\to 0}\beta\frac{\beta^3\psi_{po}(\beta) + \alpha\psi_{pm}(\beta)}{\beta^3\psi_{co}(\beta) + \alpha\psi_{cm}(\beta)}, \tag{28}$$

*Normally, in technical realization, some range at the beginning of the beam is considered as non-working.

where the dimensionless variable $\alpha = \omega^2 J_p L/EI$. Expressing the left-hand side of (28) through α and uncovering indeterminacy of the limit in the right-hand side of (28), we obtain the frequency equation

$$\frac{J_h}{J_p}\alpha - \frac{kL}{EI} = \frac{12\{3-\alpha(1-z)^2\}}{z\{12-4\alpha+\alpha z(3-z)^2\}} \tag{29}$$

in the form similar to (27). This square equation defines two different frequencies α. In the finite-dimensional (concentrated) model they corresponds to the two generalized coordinates: $v'(0,t) = \theta(t)$ and $v(L,t)$. In the limiting case of $J_h = 0$ we obtain

$$\omega^2 = \frac{12EI}{L(L-l)^2}\,\frac{3EI+kl}{12EI+kl(4L-l)/L}. \tag{30}$$

For the other limiting case, when $J_p = 0$, we have

$$\omega^2 = \frac{3EI+kl}{J_h l}. \tag{31}$$

As we can see, in this case the sensing curve is simple hyperbola giving a unique solution for the contact point.

4 Discussion

Here in this section, we want to specify and briefly discuss some theoretical and practical problems, related to and resulting from our dynamic model of the sensor under consideration.

First of all we would like to draw a parallel between the static and dynamic cases of the active sensing. For the simplicity, we consider the limiting case of a massless beam with $k = 0$. The coordinate of the contact point is defined as

$$l = 3EI\frac{\Delta\theta}{\Delta\tau_h} \tag{32}$$

for the static case [1], and

$$l = 3EI\frac{1}{J_h\omega^2} \tag{33}$$

for the dynamic case. As can be seen, in both the cases it is proportional to the impedance, with the same coefficient of proportionality. Thus, the theory of active sensing is extended from the static case to the dynamic case most logically if we allow the joint of the beam to move during the sensing process.

Next important remark is about practical realization. Of course, it is a big advantage that with the active compliant control law we can obtain, within the working range of the sensor, the single-valued sensing curve. The price we have to pay for that is stricter requirements to the driving system, especially with respect to friction. If the friction cannot be reduced to a low level and the driving system cannot be considered as perfect, the passive sensing strategy would be more appropriate.

Finally, we would like to make a comment on the future research. In our work simple contact constraints were assumed. We did not take into account possible sliding between the object and the beam and ignored the longitudinal force created by friction. It will be of interest to test how these factors influence the sensing curve. For this purpose our mathematical model must be modified, and in this connection the formalizm of contact and grasp developed in [11] can be useful.

5 Conclusions

Theoretical study of a dynamic active antenna sensor for locating a contact point has been undertaken in this paper. The study was motivated by the necessity to "improve" the frequency-contact point sensing curve by removing its multivalence region or shifting it to a non-working range. Instead of designing a special mass and stiffness distribution for the antenna, which may or may not lead to an acceptable solution, we have proposed to modify the sensing strategy itself. This is done by means of simple control actions during the sensing process. To investigate the problem at hand, the dynamic model of a flexible beam in contact with environment has been developed, and the corresponding frequency equation has been analyzed. It has been shown that the sensing curve can be a single valued function in the working range of the sensor. The solution found relaxes severe time restrictions for the measurement, simplifies the identification procedure, and reduces the number of sensor units mounted on the antenna.

References

[1] M. Kaneko, "Active Antenna," in *Proc. IEEE Int. Conference on Robotics and Automation*, May, 1994, San Diego, California, USA, Vol. 2, pp. 2665–2671.

[2] M. Kaneko, N. Ueno, and T. Tsuji, "Active Antenna: Basic Considerations on the Working Principle," in *Proc. IEEE/RSJ Int. Conference on Intelligent Robots and Systems, IROS'94*, September, 1994, Munich, Germany, Vol. 3, pp. 1744–17509.

[3] M. Kaneko, N. Kanayama, and T.Tsuji, "3-D Active Antenna for Contact Sensing," in *Proc. IEEE Int. Conference on Robotics and Automation*, May, 1995, Nagoya, Aichi, Japan, Vol. 1, pp. 1113–1119.

[4] N. Ueno and M. Kaneko, "Dynamic Active Antenna: A Principal of Dynamic Sensing," in *Proc. IEEE Int. Conference on Robotics and Automation*, May, 1994, San Diego, California, USA, Vol. 2, pp. 1784–1790.

[5] N. Ueno and M. Kaneko, "On a New Contact Sensing Strategy for Dynamic Active Antenna," in *Proc. IEEE Int. Conference on Robotics and Automation*, May, 1995, Nagoya, Aichi, Japan, Vol. 1, pp. 1120–1125.

[6] N. Ueno, M. Kaneko, and M. Svinin, "Theoretical and Experimental Investigation on Dynamic Active Antenna," submitted to the *IEEE Int. Conference on Robotics and Automation*, April, 1996, Minneapolis, Minnesota, USA.

[7] W.J. Book, "Controlled Motion in an Elastic World," *Trans. ASME, Journal of Dynamic Systems, Measurement and Control*, 1993, Vol. 115, pp. 252–261.

[8] F.L. Hu and A.G. Ulsoy, "Dynamic Modeling of Constrained Flexible Robot Arms for Controller Design," *Trans. ASME, Journal of Dynamic Systems, Measurement and Control*, 1994, Vol. 116, pp. 56–65.

[9] F. Matsuno, K. Wakashiro, and M. Ikeda, "Force Control of a Flexible Arm," in *Proc. IEEE Int. Conference on Robotics and Automation*, May, 1994, San Diego, California, USA, Vol. 3, pp. 2107–2112.

[10] B.V. Chapnik, G.R. Heppler, and J.D. Aplevich, "Modeling Impact on a One-Link Flexible Robotic Arm," *IEEE Trans. on Robotics and Automation*, 1991, Vol. RA-7, No. 4, pp. 479–488.

[11] D.J. Montana, "The Kinematics of Contact and Grasp," *The Int. Journal of Robotics Research*, 1988, Vol. 7, No. 3, pp. 17–32.